Journal of International Scientific Publication:
Materials, Methods & Technologies, Volume 3

CORROSION SYSTEMS OF IRON ARCHAEOLOGICAL ARTEFACTS

Irina Dumitriu[1,2], Radu – Claudiu Fierascu[1,2], Rodica-Mariana Ion[1,2]
and Mihaela – Lucia Ion[3]
[1] National Research & Development Institute for Chemistry and Petrochemistry – ICECHIM,
Spl. Independentei, 202, sect. 6, Bucharest, Romania
[2] Valahia University, 2 Carol I Bd, Targoviste, Romania
[3] University of Bucharest, Art History Faculty, 36-46, M. Kogalniceanu Bd, Bucharest, Romania.
E-mail: dumitriu.irina@yahoo.com

Abstract

The corrosion of archaeological artefacts in soil has been studied for different purposes. On one hand it provides information for preventing degradation of the object after excavation and ensuring its reliable restoration. On the other hand, some authors considered archaeological artefacts as analogues for the estimation of iron corrosion behaviour in soil, particularly to obtain average corrosion rates. For instance, it seems that the cathodic reaction location can move in the corrosion scale during the corrosion process.

Key words: *iron artefacts, corrosion system*

1. INTRODUCTION

Deterioration after excavation of archaeological iron artefacts buried in soil is often associated with the presence of Cl-containing phases in corrosion products, leading to serious problems for conservation of metallic objects of cultural heritage. Thus, in order to better understand the corrosion process related to the presence of chlorine, some high-resolution techniques of materials characterisation are implemented.

One of the main problems linked to the conservation of ferrous archaeological artefacts is due to the presence of chlorinated phases in the corrosion products. In fact, with environmental changes after excavation, the brutal break of the equilibrium established during artefacts burial, caused by oxygen supply, results in accelerated and destroying corrosion processes [1,2]. The fast artefact degradation following these processes is irremediable: cracking, swelling of the corrosion layers, which cause separation between the corrosion products and the iron core that can rapidly conduct to the complete loss of several hundred years old artefacts. This phenomenon occurs not only on the ferrous artefacts corroded in marine environment but also on artefacts corroded in soil. Up to now, despite relatively numerous studies on desalinisation treatment improvement [3,4] or on specific synthesised Cl-containing phases as akaganeite β-FeOOH [5,6], very few are dedicated to the fine characterisation of Cl containing corrosion products developed during the burial of archaeological artefacts and to the mechanisms at the origin of their formation. Indeed, it will be very dificult to optimise desalinisation process without a good knowledge of the nature and the location of these phases within the corrosion layers. Consequently, it is essential to apprehend the corrosion mechanisms related to the formation and evolution of Cl-containing phases in soil. It deals with the analytical characterisation of the corrosion system formed during burial. The way to obtain all physical and chemical parameters on

such corrosion products must be based on precise studies on recently excavated archaeological iron artefacts, which will be presented in this paper. Let us briefly review the literature dealing with iron aqueous corrosion in the presence of Cl ions. Refait et al. [7,8] tested the evolution of iron oxides and oxyhydroxides in different conditions depending on the pH, the level of dissolved O_2 and the Cl^- and other ion concentrations. The proportion of involved species is expressed as follows: $R=[Fe^{2+}]/[OH^-]$ and $R'=[Cl^-]/[OH^-]$. In the case of $1<[Cl^-]<1.5$mol/L, the Fe^{2+} ions present in the solution lead in a first stage to the formation of $Fe(OH)_2$ if $R'<1$ or $Fe_2(OH)_3Cl$ if $R'>1$. Once $Fe(OH)_2$ or $Fe_2(OH)_3Cl$ has precipitated, they are easily oxidised by dissolved oxygen and forms intermediate Fe(II)–Fe(III) compounds as green rust (GR). If $4<R'<8$, the final oxidation products are goethite (α-FeOOH) and akaganeite. If $R'>4$, the final product is only akaganeite. As shown by Refait [7,8] and firstly by Keller [9], Mackay [10] and confirmed by Misawa [11], akaganeite could also be obtained by the dry oxidation of the ferrous hydroxychloride β-Fe2(OH)3Cl. Indeed, only few works relate to this latter compound. However, Oswald and Feiknecht [12] established that this hydroxychloride crystallise in an hexagonal–rhombohedral structure, isomorphic with $Co_2(OH)_3Cl$ and paratacamite $Cu_2(OH)_3Cl$. It is important to note that, considering these studies, ferrous Cl-containing compounds only form in case of high concentration of Cl^-. Unfortunately, none of these studies provides detailed data on the thermodynamic stability domain of the Cl-containing phases. It is certainly due to the fact that the free formation enthalpies are not well known for some compounds or can vary with the chlorine amount. As far as archaeological ferrous artefacts are concerned, the general corrosion layout in aerated soils was described by Neff et al. [13,14]. This layout observed on a cross section of the sample is made of successive layers. The metal core of archaeological iron objects is normally covered by dense products layers (DPL), which is constituted by iron oxides and oxyhydroxides and appears relatively dense, compared to the more external layers. DPL‘ S goethite matrix. A more external layer is named by these authors transformed medium (TM). This contains simultaneously corrosion products and exogeneous compounds from the environment such as quartz grains. These authors also proposed a mechanism to explain this layout. Goethite is a non-conductive phase and maghemite or magnetite marbling seems to be non-connected to the metal core. Thus, both the cathodic reaction of oxygen reduction ($O_2+2H_2O+4e^- =4OH^-$) and the anodic reaction of iron oxidation ($Fe \rightarrow Fe^{2+}+2e^-$) take place at the interface between the remaining metal and the DPL. The new corrosion products can precipitate at the metal/ DPL interface or in the cracks depending on O_2 and pH condition, after ions migration within the pores. Vega et al. [15], confirm this hypothesis in a study using isotopic markers. Unfortunately, no precise information is available in the literature concerning the Cl-containing phases and their location in the corrosion products of archaeological artefacts buried in soil. As far as Cl-containing phases are concerned, the main part of the studies already performed on archaeological artefacts deal with objects from marine environment. However, some studies report the presence of the oxyhydroxide akaganeite β-FeOOH [16–19]. This phase is also known to form continuously after excavation even in the controlled atmosphere of museum [2]. To our knowledge, the ferrous hydroxychloride β-$Fe_2(OH)_3Cl$ was rarely identified in the iron corrosion products of iron archaeological artefacts buried in soil despite being the possible precursor of akaganeite. In order to explain the presence of chloride species within the corrosion layers, Turgoose [2] and Weizhen [20] suggest that the surface of the buried iron is gradually covered with insoluble corrosion products and then becomes further passivated. The consequence is that the anodic and cathodic reactions are separated. The oxygen is reduced when it reaches the outer conducting surface and the iron metal is oxidised in Fe^{2+}. At the iron surface, iron(II) dissolves, accumulates and can induce hydrolysis ($Fe^{2+}+H_2O \leftrightarrow Fe(OH)^+ + H^+$), which causes local acidification. Electroneutrality must be maintained to balance this charge of Fe^{2+} and H^+ cations. At this stage Selwyn et al. [1,3] consider an accumulation of chloride ions in the corrosion products. Indeed, chloride ions have a high mobility and are often the predominant environmental anions. Thus, they can diffuse from the surrounding soil and become trapped in crevices or pores of the corrosion products. According to Turgoose [2] the pores and cracks

are then filled with an acidic iron(II) chloride solution, with the Cl- ions concentrated at the metal surface. This hypothesis of cathodic reaction delocalised in the corrosion products is in contradiction with the one of Neff et al. [14] and Vega et al. [15] and has to be confirmed. Some authors were also interested by the influence of Cl on the corrosion mechanism after excavation. During this stage, the equilibrium break that occurs is connected to three factors: the O_2 concentration that is higher compared to the O_2 concentration in a burial environment, a changing relative humidity (RH) and the presence of salts as chlorides species. Askey et al. [21] developed a model of chloride corrosion cycle where Cl^- ions play a direct role in the process. During this cycle, the formation of oxyhydroxides, more precisely akaganeite, can cause physical damages to the shape of the iron object by causing stresses and cracks since the volume of those compounds is much higher than these of the previous corrosion products. This hypothesis induce that akaganeite form only after excavation time as suggested by Turgoose and Selwyn [1–3], but it was never demonstrated by archaeological artefact precise studies. It is also suggested that chemical damages are caused by the formation of HCl [21] during cycle.

This short literature review shows that no precise information can be found on the nature and location of the Cl^-containing phases formed on archaeological ferrous artefacts during burial. This lack of data can be explained because in most cases, corrosion studies on iron archaeological artefacts are only performed using investigation methods at the macroscopic scale (XRD or Mössbauer). Because of the thickness of the corrosion product, it could be difficult to detect very localised chlorinated phases in rust powders sampled on the artefact. For this reason, analyses have to be carried out with a microbeam on transverse sections, in order to locate as well as possible, at the micrometric scale, all the phases constituting the corrosion products. Moreover, as far as corrosion mechanisms are concerned, several points have to be clarified particularly the way of the Cl containing phase formation.

2. EXPERIMENTAL

2.1 Preparation of specimen

The specimens were grey cast iron, so the corrosion process would be the same as that observed in the field. The chemical composition of cast iron simulating archaeological iron is C 3.00, Si 1.84, S 0.089, P 0.097, Mn 0.083, balance is Fe. The specimens were 70mm x 30mm x 2mm. They were grounded with 150-grit silicon carbide paper and finished with 600-grit paper. Then the specimens were ultrasonically washed in acetone and methanol and dried quickly and kept in a inert atmosphere prior to the test.

2.2 Periodic wet-dry test

The periodic wet-dry tests were performed in three 1L flasks with 0.002M NaCl+ 0.008M $NaNO_3$, 0.005M NaCl + 0.005M $NaNO_3$, and 0.01M $NaNO_3$, aqueous solution respectively at 35°C , and consisted in alternating wet periods of l0 min (in solution) and *dry* period of 50min (ambient temperature). The corrosion rate was calculated by weight loss measurement at periods of 24, 48, 72 and 84 cycles. Three specimens were taken out each time and then were rinsed with distilled water, degreased and scrubbed with cotton balls to remove the corrosion products. The remaining of the corrosion products was immersed in 50% H_2SO_4 at ambient temperature. In the end, the specimens were dried in oven at 80°C for one hour, and weighed to 0.l mg.

3. RESULTS AND DISSCUSION

3.1 Weight loss measurements

Corrosion of the cast iron simulated iron artifacts were determined by using weight loss measurement. Weight losses were only recorded when the specimen had already been uniformly corroded. Variation of the weight-loss in 0.005M NaCl+ 0.005M $NaNO_3$, 0.002M NaCl+ 0.008M $NaNO_3$, and 0.01M $NaNO_3$ aqueous solution during periodic wet-dry tests is shown in figure 1.

The corrosion data are observed to approximately following the well-know bilogarithmic equation

$$C=At^B \quad (1)$$

where C is the weight loss (g), t is the periodic test time (h), A and B are constants. It is clear that the value of A is equals to the weight loss in the unit time. B reflects the changes of weigh loss with time. Table 1 lists the regression coefficients of the corrosion data from the weight-loss method. It is clearly observed from figure 1, the corrosion rate induced by $NaNO_3$ is the lowest during the corrosion process of the test and drop notably as time going on. With the addition of NaC1, the corrosion rate of specimen increases. However corrosion rates induced by $NaNO_3$+NaCl do not drop so fast as corrosion proceeds. It is well known that constant B is roughly equal to 0.5 of the corrosion which is controlled by an ideal diffusion process; if the value of B is smaller than 0.5, it means a decrease in diffusion coefficient and the rust layer become more protective. Thus the rust layer induced by $NaNO_3$, is more protective than that induced by $NaNO_3$+NaCl according to the value of B shown in Table 1.

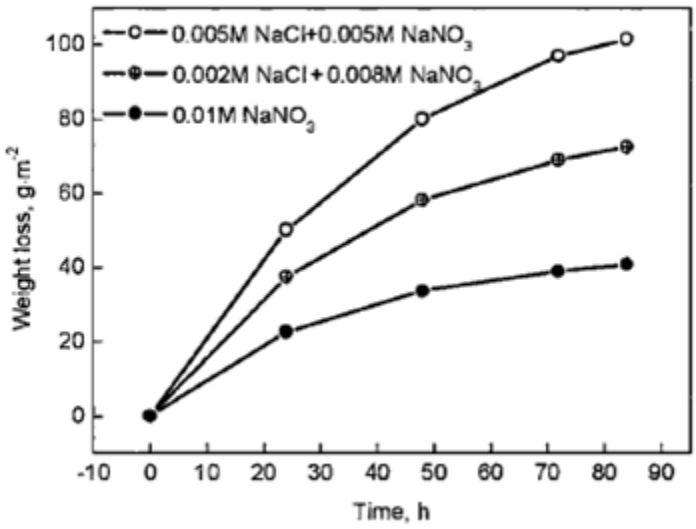

Figure 1 Weight loss curves induced by three aqueous solutions in periodic wet-dry test.

Table 1 The regression coefficients of the corrosion data from weight-loss measurements

Solution	**A**	***B***
0.005M NaCl + 0.005M $NaNO_3$	9.66498	0.49183
0.002M NaCl + 0.008M $NaNO_3$	7.84415	0.50145
0.01M $NaNO_3$	5.97812	0.40229

3.2 Surface analysis

Generally speaking, rust has important effects on the subsequent corrosion rate. Weeping ("yellow beads of liquid or brown globules of liquid") was observed clearly which may be due to the present of Cl^-. However, the phenomena didn't appear in the specimens immersed in $NaNO_3$ solutions and it exhibits a uniform and compact corrosion layer. In contrast, the rust layers induced by Cl^- demonstrate a more severe attack on the rust layer. To analyze the effects of the rust layer, SEM analysis was used for identifying the constituents of rust layer formed on the specimens after the periodic wet-dry test. SEM analysis of the samples after periodic test in the three different solutions are showed in figures 2-4. SEM micrographs show that attacks on the specimen induced by 0.002M NaC1+ 0.008M $NaNO_3$ and 0.005M NaCl + 0.005M $NaNO_3$ environment are stronger than that induced by $NaNO_3$ environments. When C1- ions are in present of the solution, the rusted layers of the specimen seemed to be much rougher than that induced by the $NaNO_3$ solution. This is one of the reasons why the corrosion rate at the late period is higher than that induced by $NaNO_3$ solution.

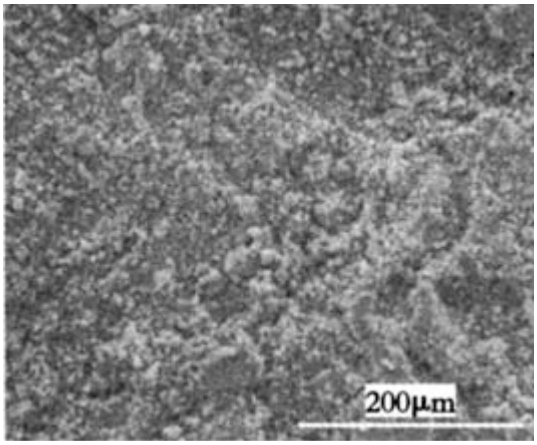

Figure 2. SEM micrograph of rusted sample induced by $NaNO_3$ after periodic wet-dry test.

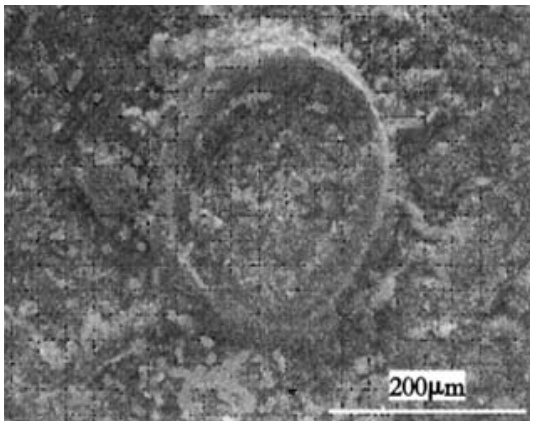

Figure 3. SEM micrograph of rusted sample induced by 0.008M $NaNO_3$+0.002M NaCl after periodic wet-dry test.

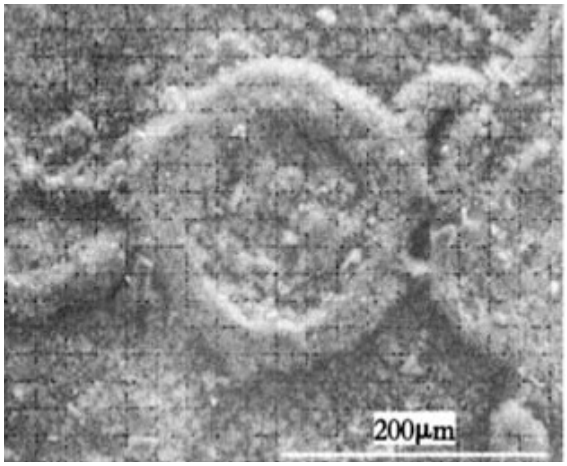

Figure 4. SEM micrograph of rusted sample induced by 0.005M $NaNO_3$+0.005M NaCl after periodic wet-dry test.

It can also be seen that there are wide pits observed in figures 3 and 4 which is the relic of the "weeping".

3.5 Corrosion mechanisms

As showed by the weight loss measurement results, the corrosion rate induced by NO_3^- is the lowest at the initial stage of corrosion. This may be due to the following reasons: First, the surface activity of NO_3^- is the low. Second, as a strong oxidizer, the HNO_3 produced during the corrosion process can oxidize Fe into Fe^{3+} directly, which inhibits the formation of the Fe^{2+} state. The concentration of the Fe^{2+} on the outermost part of the oxide surface could determine the kinetics of 0, reduction. This may be due either to the formation of catalytic active complexes between Fe^{2+} ions and the oxygen molecule or due to chemical reduction of oxygen by the Fe^{2+} followed by an electrochemical reduction of the Fe^{3+} generated during the chemical reactions. O_2 reduction reaction is more likely to take place where the mount of Fe^{2+} is high. Few Fe^{2+} exist during the corrosion process which doesn't favor the reduction of oxygen. This is another reason why the corrosion rate of iron in NO_3^- bearing pollutants is

the lowest in the three different environments at the initial stages. Thirdly, the uniform and compact characteristics of the rust layer together with the poor penetration ability contribute to the protection of the substrate metal. This also explains why the corrosion rate drops sharply at the later corrosion stage. The effect of $C1^-$ can be explained by an auto-catalysis process.

In addition, it had been reported [22] that $C1^-$ inhibits the phase transformation from γ-FeOOH to more stable α-FeOOH. As corrosion goes on, the attack to the substrate is still strong due to the poor protectiveness of rusted layer and the high penetration ability of $C1^-$. Thus, in the later period, the corrosion rate induced by $C1^-$ bearing pollutant was still obvious. When $C1^-$ is present in NO_3- bearing pollutants, the surface tension of electrode/solution interface decreases [23]. Corrosion on metal is more inclined to occur. Meanwhile more Fe^{2+} is produced during the corrosion process when $C1^-$ is presented in NO_3^- bearing pollutant. This promotes the dissolution of cast iron. Protection of the rust layer to substrate becomes poor. In addition, the high surface activity and high mobility of $C1^-$ accelerate the corrosion process too.

The autocatalysis effect and high mobility of $C1^-$ contribute to the formation of weeping. Meanwhile micro-cavities and cracks occur during the corrosion process. The formation of these micro-cavities and cracks is evaluated in relation to the acid produced and the formation of solid products, which could give rise to local stresses and cause the dissolution of other corrosion products, thereby chemically assisting the propagation of cracks and aiding the disintegration of the rust layers. The micro-morphology and the constituent of the corrosion products reveal good agreement with the corrosion rates at the later corrosion period estimated from the weight loss measurement. Accelerating effects of simultaneous interaction of $NaNO_3$ + $C1^-$ on grey cast iron have been observed with corrosion going on [24,25].

4. CONCLUSION

The attack of anions to the metal at the initial corrosion stage shows great agreement with their surface activity. However as corrosion goes on, the penetration effect of anions together with the different characteristics of the corrosion products come to control the corrosion process.

When minor $C1^-$ is in the present of NO_3^-, iron show accelerating effects which is chiefly due to the increasing of surface activity at the initial corrosion stage and the penetration effect of $C1^-$ at the late corrosion periods. Greater accelerating effect is observed if the content of C1- increases.

REFERENCES

1. Selwyn L.S., Sirois P.J., Argyropoulos, *The corrosion of excavated archaeological iron with details on V. weeping and akaganeite,* Studies in Conservation 44 (1999) 217–232.

2. Turgoose S., *Post-excavation changes in iron antiquities*, Studies in Conservation 27 (1982) 97–101.

3. Selwyn L.S., Argyropoulos V., R*emoval of chloride and iron ions from archaeological wrought iron with sodium hydroxide and ethylenediamine solutions*, Studies in Conservation 50 (2003) 81–100.

4. North N.A., Pearson C., *Washing methods for chloride removal from marine iron artefacts*, Studies in Conservation 23 (1978) 174–186.

5. Stahl K., et al., *On the akaganeite crystal structure, phase transformations and possible role in post-excavational corrosion of iron artifacts*, Corrosion Science 45 (2003) 2563–2575.

6. Post J.E., et al., *Neutron and temperature resolved synchrotron X-ray powder diffraction study of akaganeite,* American Mineralogist 88 (2003) 782–788.

7. Refait P., Abdelmoula M., Genin J.-M.R., *Mechanisms of formation and structure of green rust one in aqueous corrosion of iron in the presence of chloride ions*, Corrosion Science 40 (9) (1998) 1547–1560.

8. Refait P., Genin J.-M.R., *The mechanisms of oxidation of ferrous hydroxychloride _-Fe2(OH)3Cl in aqueous solution: the formation of akaganeite vs goethite*, Corrosion Science 39 (3) (1997) 539–553.

9. Keller P., *Vorkommen, Entstehung und Phasenumwandlung von beta-FeOOH in Rost*, Werstoffe und Korrosion Heft 2 (1969) 102–108.

10. Mackay A.L., *Beta-ferric oxyhydroxide, akaganeite*, Mineralogical Magazine 33 (1962) 270–280.

11. Misawa T., Hashimoto K., Shimodaira S., *The mechanism of formation of iron oxide and oxyhydroxides in aqueous solutions at room temperature*, Corrosion Science 14 (1974) 131–149.

12. Oswald H.R., Feitknecht W., *über die Hydroxidhalogenide Me2(OH)3Cl–Br, –J zweiwertiger Metalle (Me=Mg, Ni, Co, Cu, Fe, Mn),* Helvetica Chimica Acta 47 (1964) 272–289.

13. Neff D., *Apport des analogues archéologiques à l'estimation des vitesses moyennes et à l'étude des mécanismes de corrosion à très long terme des aciers non alliés dans les sols*, in: Sciences Mécaniques pour l'Ingénieur, Université de Technologie de Compiègne, Compiègne, 2003, p. 360.

14. Neff D., et al., *Corrosion of iron archaeological artefacts in soil: characterisation of the corrosion system,* Corrosion Science 47 (2005) 515–535.

15. Vega E., Berger P., Dillmann P., *A study of transport phenomena in the corrosion products of ferrous archaeological artefacts using 180 tracing and nuclear microprobe analysis*, Nuclear Instruments and Methods B 240 (2005) 554–558.

16. Zucchi F., Morigi G., Bertolasi V., *Beta iron oxide hydroxide formation in localized active corrosion of iron artifacts*. Corrosion and metal artifacts, a dialogue between conservators and archaelogists and corrosion scientists, 479, 1977, pp. 103–105.

17. Arnould-Pernot P., *Traitement de dechloruration des objets archeologiques ferreux par plasma d'hydrogene,* Institut National Polytechnique de Lorraine, Ecole des Mines de Nancy, Laboratoire de Science et Genie des Surfaces, Nancy, 1994, p. 157.

18. Rinuy A., Schweizer F., *Méthodes de conservation d'objets de fouilles en fer. Etude quantitative comparée de l'élimination des chlorures*, Studies in Conservation 26 (1981) 29–41.

19. Pons E., *Corrosion à long terme du fer et des aciers non ou faiblement alliés dans les sols à dominante argileuse* – Caractérisation Physico-chimique et étude électrochimique d'analogues archéologiques, Université de Technologie de Compiègne, Compiègne, 2002, p. 239.

20. Weizhen O., Chunchun X., *Studies on localized corrosion and dessalination treatment of simulated cast iron artifacts*, Studies in Conservation 50 (2004) 101–108.

21. Askey A., et al., *The corrosion of iron and zinc by atmospheric hydrogen chloride*, Corrosion Science 39 (1993) 539–553.

22. Cronyn J.M., *The Elements of Archaeological Conservation* (Routledge, London, 1990) p.194.

23. Selwyn L.S., Mckinnon W.R., Argyropoulos V., *Models for chloride ion diffusion in archaeological iron,* Studies in Conservation 46 (2001) 109–120.

24. Réguer S., Dillmann P., Mirambet F., *Buried iron archaeological artefacts: Corrosion mechanisms related to the presence of Cl-containing phases,* Corrosion Science 49 (2007) 2726–2744

25. Cao X., Xu C.C., *Effect of chloride on the atmospheric corrosion of simulated artefact iron in NO_3^- bearing pollutant environment,* Acta Metall. Sin. (Engl. Lett.) Vol. 19 No. 1 (2006), 34-42.